Title

PRECIPITATION AT THE TUNGSTEN-TUNGSTEN INTERFACES IN TUNGSTEN-NICKEL-IRON HEAVY ALLOYS

Authors

Posthill, J.B.
Hogwood, M.C.
Edmonds, D.V.

Publication Date

1985-05-01

Lawrence Berkeley Laboratory
UNIVERSITY OF CALIFORNIA

Materials & Molecular Research Division

Submitted to Powder Metallurgy

PRECIPITATION AT THE TUNGSTEN-TUNGSTEN INTERFACES IN TUNGSTEN-NICKEL-IRON HEAVY ALLOYS

J.B. Posthill, M.C. Hogwood, and D.V. Edmonds

May 1985

Prepared for the U.S. Department of Energy under Contract DE-AC03-76SF00098

DISCLAIMER

Precipitation at the Tungsten-Tungsten Interfaces in Tungsten-Nickel-Iron Heavy Alloys

J.B. Posthill[+], M.C. Hogwood[++] and D.V. Edmonds[+++]

[+]National Center for Electron Microscopy
Materials and Molecular Research Division
Lawrence Berkeley Laboratory
University of California
Berkeley, California 94720

[++]Materials Branch
Royal Armament Research and Development Establishment
Sevenoaks, Kent.

[+++]Department of Metallurgy and Science of Materials
University of Oxford
Oxford

Abstract

A study of precipitation at the tungsten grain boundaries in the tungsten-nickel-iron ternary alloy system has been undertaken. Scanning and transmission electron microscopy techniques have been used to study the effect of various post-sintering heat treatments on the precipitation reaction. Grain boundary precipitates with a crystal structure and lattice parameter the same as the matrix binder phase (f.c.c., a_0 = 0.360nm) have been shown to form at the tungsten grain boundaries during heat treatment in the 800 -1300° C temperature range. A mechanism for the formation of these precipitates is proposed. It has also been found that the tungsten grain boundary precipitates consistently behave in a ductile manner upon tungsten-tungsten interfacial failure. This may give an opportunity for an improvement in ductility of the inherently brittle tungsten grain boundaries in these alloys.

1. INTRODUCTION

Tungsten-nickel-iron alloys are manufactured using the standard powder metallurgical technique of hydrostatically cold pressing elemental powders followed by liquid phase sintering. During the sintering process the liquid phase of nickel and iron dissolves only some of the tungsten, while very effectively wetting the remaining solid tungsten. These solid tungsten particles then grow primarily by a process of dissolution and reprecipitation[1] although coalescence[2] also contributes to grain growth. Upon cooling the resulting microstructure consists of a semicontiguous network of spheroidal grains of tungsten (often 20-40 μm in diameter) surrounded by a face-centered cubic matrix of nickel, iron and tungsten (Fig. 1). For a 90%W-5%Ni-5%Fe alloy, the matrix composition is typically 40%Ni-40%Fe-20%W.

Although in terms of mechanical properties the tungsten grains[3] and matrix phase have a marked effect, the strength of the various interfaces is also known to be important. There are three basic types of interfaces present in the heavy alloy viz., matrix grain boundaries, tungsten-matrix interphase boundaries and tungsten grain boundaries. Because of the typically large matrix grain size ($>$ 100 μm), matrix grain boundaries are infrequently observed and hence are not expected to affect greatly the mechanical properties or the failure mechanism of the heavy alloy. Additionally, the matrix phase has consistently been found to fail in a ductile manner[4] thus lending additional support to the belief that the role of the matrix grain boundaries during alloy deformation and failure is generally negligible.

The tungsten-matrix interphase boundary behavior and microstructure is significantly more complex. In heavy alloys containing suitable amounts of carbon (i.e., $\gtrsim$ 0.01 wt% C), eta-carbide precipitation at this interface can occur during cooling from the sintering temperature[5,6] or upon post-sintering heat treatment.[6,7] It is well-known that the presence of a third phase at this interface severely embrittles the alloy.[8] Additionally, Auger electron spectroscopy performed on certain alloys showing significant tungsten-matrix interfacial failure has shown significant impurity segregation of phosphorous and sulfur to these boundaries[9,10]. This phenomenon is also associated with alloy embrittlement. Recently, the suggestion that hydrogen segregates to and embrittles the tungsten-matrix interphase boundaries has also been put forward.[11,12] The microstructure of this interface is an important parameter in determining the mechanical behavior of tungsten heavy alloys.

Somewhat surprisingly, the tungsten grain boundaries have received relatively little attention, even though tungsten intergranular failure often comprises over 50% of the fracture area. Whilst evidence for precipitation at the tungsten grain boundaries certainly exists,[10,13,14,15] little work has been done to determine the nature and morphology of precipitation and the conditions under which the reaction occurs. It is with this aim, along with the possibility of eventually improving the cohesion of the tungsten grain boundaries, that this investigation was undertaken.

2. EXPERIMENTAL PROCEDURES

The presence of a second phase at the tungsten grain boundaries was initially observed during examination of a commercially produced 95%W-3.5%Ni-1.5%Fe alloy. Accordingly, a survey of readily available commercially supplied W-Ni-Fe heavy alloys was undertaken. These alloys are listed in Table I along with their processing histories. It should be noted that certain alloys were supplied in the "as-sintered" condition whereas others were typically given a proprietary post-sintering heat treatment. For this reason it was decided to manufacture an experimental alloy under controlled, laboratory conditions.

Fine powders of commercially pure elemental tungsten, nickel and iron were weighed and then mixed together in a ball grinder for 16 hours. The blended powder was then isostatically pressed at a pressure of 275 MNm^{-2} to produce a green compact. The billet was heated to 900°C under flowing dry hydrogen and held for 1 hour. The temperature was subsequently increased to the liquid phase sintering temperature of 1450°C. After 1 hour the power to the furnace was switched off; thereby allowing the bar to cool slowly from the sintering temperature. In order to evaluate the feasibility of a combined heat treatment, some material was slowly cooled from the sintering temperature to an intermediate temperature and then held for a period of time prior to cooling slowly to room temperature.

Scanning electron microscopy was performed on fracture surfaces of the various heavy alloys created by breaking notched specimens with a sharp blow. Thin foils for transmission electron microscopy were

produced by an electropolishing technique described in detail elsewhere.[7] The standard techniques of image formation, electron diffraction and energy dispersive x-ray spectrometry were used to determine the morphology, structure and composition of the precipitate.

3. EXPERIMENTAL RESULTS

3.1 COMMERCIAL ALLOYS

Fractographic examination of both the 95%W-3.5%Ni-1.5%Fe and 90%W-5%Ni-5%Fe alloys revealed the presence of a second phase at some of the tungsten-tungsten interfaces that had failed in an intergranular manner (Fig. 2). In contrast, the 90%W-7%Ni-3%Fe and 96%W-2%Ni-2%Fe alloys showed only smooth, featureless regions of tungsten intergranular failure indicating that precipitation has not occurred at this boundary (Fig. 3). The difference in processing histories between the two sets of alloys is that the former have been given a commercial post-sintering heat treatment whereas the latter have not. Therefore, the formation of precipitates on the tungsten grain boundaries appeared to be associated with post-sintering heat treatment. This was verified by laboratory heat treatment of the 90%W-7%Ni-3%Fe and 96%W-2%Ni-2%Fe alloys at 900° C and also at 1050° C for 1 hour followed by water quenching. Both of these heat treatments did indeed induce observable precipitation at the tungsten grain boundaries (Fig. 4), although it must be strongly emphasized that regions showing precipitation were inhomogeneously located throughout the microstructure.

Several important observations concerning the details of this reaction were made by fractographic study. For example, the precipitate morphology was found to vary considerably, not only from interface

to interface on a given sample, but even on a single grain boundary surface (e.g., Fig. 2). The precipitate geometries observed ranged from fine and coarse needles to nodular particles (Fig. 5). Needle-like precipitates often showed a tendency for alignment, suggesting the existence of a specific habit direction and a crystallographic orientation relationship between the precipitate and one or both of the adjacent tungsten grains. Quite often the precipitates were seen to be greater in number but smaller in size when located nearer to the perimeter of the tungsten grain boundary (Figs. 2 and 5(c)). Additionally, there was evidence for the existence of a precipitate-free zone (PFZ) on those tungsten grain boundaries that showed precipitation. Note that the term PFZ is not used in the conventional sense. It refers to the perimeter region of a tungsten grain boundary. Only in isolated and rare cases, was a precipitate observed to be contiguous with the matrix region of the heavy alloy.

As the precipitates observed in this fractographic study have been involved in the failure process, it is interesting to note their behavior. For the most part, the precipitates deformed to some extent during alloy failure, thus indicating their intrinsic ductility. However, the adhesion between the precipitate and tungsten grains appeared to vary. Sometimes a precipitate became detached during failure leaving only depressions on the tungsten grain boundary surface (Fig. 5(c)). These precipitates presumably adhered to the corresponding tungsten grain on the fracture surface not shown in this particular case. Nevertheless, the majority of tungsten grain boundary surfaces displaying a topography indicative of precipitation did show a certain

amount of actual precipitate material present. This implies that in most cases the fracture path proceeds through the interior of the ductile precipitates when present.

Transmission electron microscopy was used to ascertain the crystal structure and approximate composition of the interfacial precipitate phase. Figure 6 shows typical TEM bright and dark field precipitate images that were obtained at 100 KeV. At this accelerating voltage it was not possible to obtain complete, indexable selected area electron diffraction patterns from the precipitate phase. However, all single diffraction spots from many different precipitates in the various alloys were found to be consistent with the precipitate having a face-centered cubic structure with lattice parameter, a_o = 0.360 nm, which is essentially identical to that of the matrix phase. More complete selected area electron diffraction patterns were obtained at higher accelerating voltage (1 MeV) that confirmed this result. Comparative thin film EDS spectra are displayed in Figure 7. As can be seen the precipitate contains significant amounts of nickel, iron and tungsten roughly similar to the matrix phase. Clearly, these results show that the interfacial precipitate phase is the same as the matrix phase, although the precise compositions may differ.

Electron microdiffraction was used in an attempt to determine the crystallographic orientation relationship between the f.c.c. precipitate and the adjacent b.c.c. tungsten grains. Unfortunately, experimental circumstances prevented extensive analyses of a statistically significant number of precipitates. Nevertheless, preliminary results have shown that no rational orientation relationship

exists between the interfacial precipitate phase and either adjacent tungsten grain. In one case it was found that the precipitate was oriented between the well-known Nishiyama-Wassermann[16,17] (N-W) and Kurdjumov-Sachs[18] (K-S) b.c.c./f.c.c. orientation relationships with *both* adjacent tungsten grains. This is shown in Figure 8 alongside the microdiffraction evidence. One grain is oriented three degrees from K-S (towards N-W) with the precipitate whereas the other is oriented three degrees from N-W (towards K-S). As the N-W and K-S orientation relationships differ by a 5.26° rotation about the normal to the (parallel) close-packed planes, it is clear that the precipitate has an identical orientation relationship with each adjacent tungsten grain within an experimental error of approximately one degree. It should also be noted that a set of close-packed planes in each of the three crystals are mutually parallel. In another case the precipitate was not found to be oriented near (i.e. within 10°) a rational orientation relationship with one of the adjacent tungsten grains. Nevertheless, the precipitate and the other adjacent tungsten grain were oriented within the 10.8° "orientation region" consistent with the Bain correspondence[19] as determined by Ryder and Pitsch[20].

3.2 EXPERIMENTAL ALLOY

A batch of tungsten heavy alloy was produced under laboratory conditions having nominal composition 90%W-5%Ni-5%Fe. Examination of the fracture surface of this alloy after sintering failed to reveal the presence of tungsten-tungsten interfacial precipitation; however, a few tungsten grain surfaces did contain regions of entrapped matrix, which is distinct from precipitation (Fig. 9). This feature is not

uncommon and may be expected to occur occasionally as a result of irregular tungsten grain growth and impingment during liquid phase sintering.

Isochronal heat treatments (t = 1 hour) in the temperature range 700 -1300°C were conducted on this alloy. After heat treatment at 700°C the tungsten grain boundary surfaces appeared featureless indicating the absence of precipitation. At 800°C extremely fine, elongated depressions on the failed interfaces were observed (Fig. 10). These depressions were always seen near to the perimeter of the grain boundary surface although they were not observed to be contiguous with the matrix region. Fine rod-like precipitates were the most common feature of the sample heat treated at 900°C. Again, this morphology was observed near the perimeter of the grain boundary surface. Annealing at 1050°C produced very mixed precipitate morphologies; coarser precipitates and both rod-like and nodular morphologies were observed. A further increase in temperature to 1300°C resulted in very little observable precipitation although some nodular and short rod-like precipitates were infrequently detected. As in the case of the commercial alloys, the extent of the reaction was quite limited and sporadic.

A series of isothermal heat treatments were conducted at 1050°C for times ranging from 40 minutes to 24 hours. As expected, examination of the sample aged for 40 minutes revealed precipitation predominantly in the shape of fine elongated rods; however, some areas did exhibit small nodular precipitates. At longer aging times, up to 24 hours, precipitation was found to be much coarser with a nodular

morphology predominating. In addition to the precipitates being larger, it appeared that many more depressions on the failed tungsten interfaces were observed suggesting that the precipitate-tungsten boundary adhesion had decreased with prolonged aging. A sample was heat treated for 100 hours at 800 °C to compare with the precipitation observed after 1 hour at 800 °C (Fig. 10(a)). Precipitation was observed on considerably more boundaries and was found to be significantly coarser although still rod-like in nature (Fig. 10(b)). Generally, the precipitate dimensions increased predominantly in the plane of the boundary during growth, although some thickening did occur normal to the boundary.

The normal cooling process from the sintering temperature was altered for some samples to examine the effect this might have on tungsten grain boundary precipitation. The slow cooling was interrupted by holding specimens at 800°C and 1050°C, respectively, for times ranging from 1 hour to 100 hours before subsequently cooling to room temperature. Examination of the fracture surfaces did not show any evidence for tungsten grain boundary precipitation. These same samples were then given an additional 1 hour at 1050°C which, interestingly, did produce precipitation in the normal manner. It appears that cooling to a lower temperature is essential if subsequent aging is to produce the observed precipitation reaction.

4. DISCUSSION

The grain boundary precipitates have been shown to be face-centered cubic with lattice parameter a_0 = 0.360 nm and contain nickel, iron and tungsten as their principal elemental constituents. This is directly comparable with the f.c.c. matrix binder phase (γ -phase). A

post-sintering heat treatment in the 800-1300°C temperature range after first cooling to a lower temperature is essential for the observation of this reaction at the tungsten grain boundaries.

The observed precipitate morphology offers certain clues as to the mechanism of the reaction. For example, the precipitate-free zone around the perimeter of a tungsten grain boundary appears to suggest that the driving force for the reaction is the supersaturation of nickel and iron in the tungsten grains at the aging temperature. It would be expected that the tungsten phase would contain some quantity of nickel and iron when the nature of tungsten grain growth during liquid phase sintering at 1450° C is considered. This is substantiated by electron microprobe data that clearly shows the tungsten grains to contain 0.1 at % nickel and 1.1 at % iron after fabrication[21]. Of course, γ-phase precipitates are not observed at the tungsten-matrix interphase boundaries because the matrix is the same phase. Interestingly, however, there is evidence of a "zone" in the matrix phase adjacent to the tungsten grains.[22] This "zone" appears brighter than the rest of the matrix when viewed in the TEM and one possible interpretation is that it represents a tungsten-poor (or, nickel- and iron-rich) region produced during heat treatment.

Another possible source for nickel and iron is the matrix region. For nickel and iron to diffuse up the tungsten grain boundaries and subsequently precipitate would require an appropriate thermodynamic driving force. It appears unlikely that this would afford a substantial reduction of chemical free energy or a reduction in strain energy. In fact, the strain energy would most certainly increase. This leaves

only the lowering of the total interfacial free energy as a possible driving force consistent with this mechanism. However, the observed PFZ would be an unlikely result of the replacement of a tungsten grain boundary with two W-γ interphase boundaries. Additionally, the presence of **discrete** precipitates on the grain boundaries automatically implies a balance of the respective interfacial energies.[23] Consequently, the available evidence supports the contention that nickel and iron precipitate from the supersaturated tungsten grains in the 800-1300° C temperature range to form the nickel, iron and tungsten-containing γ-phase precipitates at the tungsten grain boundaries.

The inhomogeneous nature of this reaction can be interpreted as being due to small chemical fluctuations in the amounts of nickel and iron from one tungsten grain to another. Both the equilibrium nickel and iron solubilities in tungsten are thought not to vary profoundly with temperature between the liquid phase sintering temperature (1450° C) and the lowest aging temperature at which grain boundary precipitation is observed (800° C).[24] As a result small differences in the nickel and iron concentrations in the tungsten grains would be expected to alter drastically their respective levels of supersaturation. It is plausible that precipitation could be suppressed locally by a small reduction in nickel and iron concentration in a particular tungsten grain. Another possibility is that certain impinging tungsten grains are crystallographically oriented in such a way as to allow a precipitate embryo to establish a low energy configuration consisting of simultaneously optimizing the orientation relationships and habit planes (or directions) with both adjacent grains. Precipitation would then

be preferred at such boundaries because of the reduction in the critical free energy for nucleation. Preliminary electron diffraction evidence indicated that this tendency might exist for tungsten grain boundaries in which a set of {110} planes in each crystal are parallel. However, further experimental research would be necessary to decide which of the above mechanisms correctly describes the sporadic nature of this precipitation reaction.

It remains to be shown systematically and quantitatively just how much this precipitate morphology will affect mechanical properties. However, the ductile precipitates should, if they adhere to both tungsten grains, improve the cohesion of the inherently brittle tungsten grain boundaries. This is partially borne out by the works of Brandon et al.[13] and Gero and Chaiat[15] which claim that an increase in ductility is conferred by precipitation at the tungsten grain boundaries. These γ-phase precipitates would certainly reduce the total tungsten grain boundary area which, as Muddle and Edmonds[9] suggest, may in itself increase the impact resistance of the heavy alloy.

5. CONCLUSIONS

Precipitation of a nickel, iron and tungsten containing phase at the tungsten grain boundaries has been observed in a number of W-Ni-Fe alloys when aged in the 800-1300° C temperature range. This phase is the same as that of the matrix binder phase - both are f.c.c. with lattice parameter, a_0 = 0.360nm. It is believed that this reaction occurs by precipitation of nickel and iron from the supersaturated tungsten grains. The precipitates generally behaved in a ductile manner during tungsten intergranular failure and are believed to improve the

cohesion at these boundaries. Although the extent of precipitation is limited and sporadic, it is thought that this reaction can be exploited to enhance the mechanical properties of tungsten-nickel-iron heavy alloys.

6. ACKNOWLEDGEMENTS

The authors gratefully acknowledge Professor Sir Peter Hirsch F.R.S. for the provision of laboratory facilities at Oxford University. The authors are also indebted to Mr. J. Markham (RARDE) for his assistance with scanning electron microscopy. This work has been carried out with the support of the Procurement Executive, Ministry of Defence. One of us (JBP) acknowledges support by the Director, Office of Energy Research, Office of Basic Energy Sciences, Materials Sciences Division of the U.S. Department of Energy under Contract No. DE-AC03-76SF00098 during manuscript preparation.

7. REFERENCES

1. G.H.S. Price, C.J. Smithells and S.V. Williams, J. Inst. Metals, 62, 239 (1938).
2. E.G. Zukas and H. Sheinberg, Powder Technology, 13, 85 (1976).
3. J.B. Posthill and D.V. Edmonds, Mat. Res. Soc. Symp. Proc., 21, 811 (1984), Ed. T. Tsakalakos.
4. M.C. Hogwood, unpublished research, R.A.R.D.E., Sevenoaks, Kent.
5. B.C. Muddle, Metall. Trans. 15A, 1089 (1984).
6. B.C. Muddle and D.V. Edmonds, to be published.
7. J.B. Posthill and D.V. Edmonds, to be published.
8. D.V. Edmonds and P.N. Jones, Metall. Trans., 10A, 289 (1979).
9. B.C. Muddle and D.V. Edmonds, Metal Science, 17, 209 (1983).
10. C. Lea, B.C. Muddle and D.V. Edmonds, Metall. Trans., 14A, 667 (1983).

11. Z. Guisen, L. Mingcheng, L. Zhongjie and Y. Shuyan, Acta Metall. Sinica, 17, 39 (1981).

12. H.K. Yoon, S.H. Lee, S.-J. L. Kang and D.N. Yoon, J. Mat. Sci., 18, 1374 (1983).

13. D.G. Brandon, E. Ariel and J. Barta, Proc. 5th Int. Symp. Electron Microscopy and Structure of Materials, 849 (1972), Ed. G. Thomas.

14. I.N. Frantsevich, R.V. Minakova and L.G. Bazhenova, 5th Polish Conf. on Powder Metallurgy, 2, 221 (1979).

15. R. Gero and D. Chaiat, Materials Enginering Conf., 46 (1981) Haifa, Isreal.

16. Z. Nishiyama, Sci. Rep. Res. Inst. Tôhoku Univ., 23, 638 (1934).

17. G. Wassermann, Arch. Eisenhütt Wes., 16, 647 (1933).

18. G. Kurdjumov and G. Sachs, Z. Phys., 64, 325 (1930).

19. E.C. Bain, Trans. Metall. Soc. A.I.M.E., 70, 25 (1924).

20. P.L. Ryder and W. Pitsch, Acta Metall., 14, 1437 (1966).

21. J.B. Posthill, D. Phil. Dissertation, University of Oxford (1983).

22. B.C. Muddle and D.V. Edmonds, unpublished research.

23. P.J. Clemm and J.C. Fisher, Acta Metall., 3, 70 (1955).

24. W.G. Moffatt, The Handbook of Binary Phase Diagrams, General Electric Company (1978).

TABLE 1

COMPOSITION AND HISTORY OF COMMERCIAL ALLOYS

NOMINAL COMPOSITION	PROCESSING HISTORY
95W - 3.5Ni - 1.5Fe	SINTERED + POST-SINTER HEAT TREATMENT
90W - 5Ni - 5Fe	SINTERED + POST-SINTER HEAT TREATMENT
90W - 7Ni - 3Fe	SINTERED
96W - 2Ni - 2Fe	SINTERED

8. FIGURE CAPTIONS

Fig.1 Optical micrograph of sintered and heat treated 90W-5Ni-5Fe alloy.

Fig.2 Scanning electron micrograph of fracture surface of commercial 95W-3.5Ni-1.5Fe alloy in sintered and heat treated condition.

Fig.3 SEM micrograph of fracture surface of commercial 96W-2Ni-2Fe in the as-sintered condition.

Fig.4 Same alloy as Figure 3 after a post-sintering heat treatment for 1 hour at 1050° C.

Fig.5 Various precipitate morphologies observed; (a) elongated rods, (b) nodular, (c) depressions on grain surface containing some precipitate material.

Fig.6 TEM micrographs of a grain boundary precipitate in a commercial 95W-3.5Ni-1.5Fe alloy; (a) bright field, (b) dark field using an f.c.c. reflection, (c) selected area electron diffraction pattern.

Fig.7 Energy dispersive x-ray spectra from; (a) tungsten grain, (b) matrix binder phase, (c) tungsten grain boundary precipitate.

Fig.8 Electron microdiffraction patterns showing the orientation relationships between a grain boundary precipitate and both tungsten grains. They are different variants but equivalent and are expressed relative to rational f.c.c. indices.

Precipitate(a)		W(b)		W(c)
$[\bar{1}01]$	//	$[.\overline{89}, \bar{1}, 1]$	//	$[.\overline{04}, .04, 1]$
$[111]$	//	$[011]$	//	$[110]$
$[\bar{1}2\bar{1}]$	//	$[\overline{2.24}, 1, \bar{1}]$	//	$[\bar{1}, 1, .\overline{07}]$

Fig. 9 SEM micrograph of fracture surface of experimental 90W-5Ni-5Fe alloy in the as-sintered condition showing a region of entrapped matrix.

Fig.10 SEM micrographs of fracture surface of experimental alloy after; (a) 1 hour at 800°C showing extremely fine, elongated depressions, (b) 100 hours at 800°C showing much coarser precipitates.

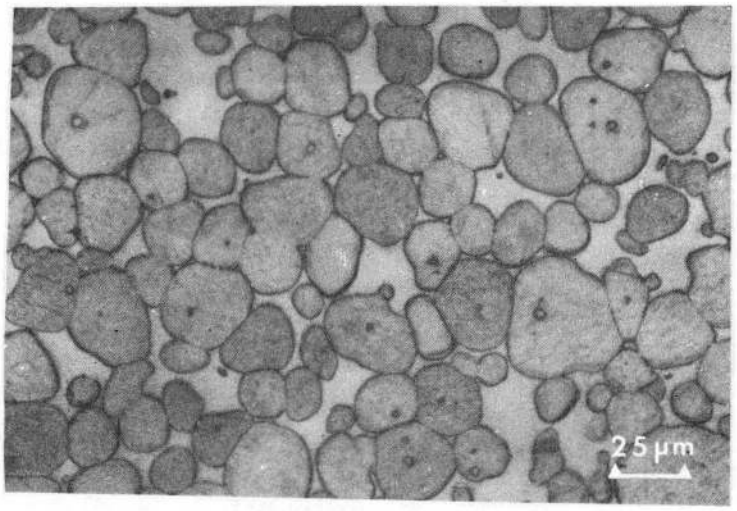

Fig. 1

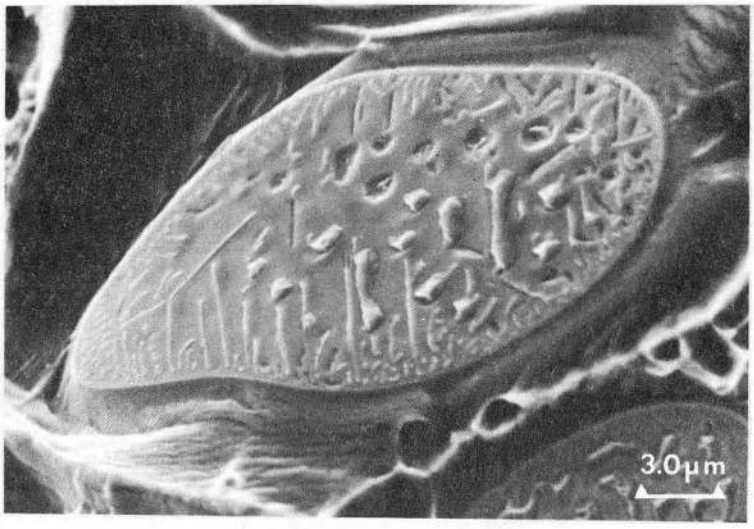

Fig. 2

XBB 855-4067

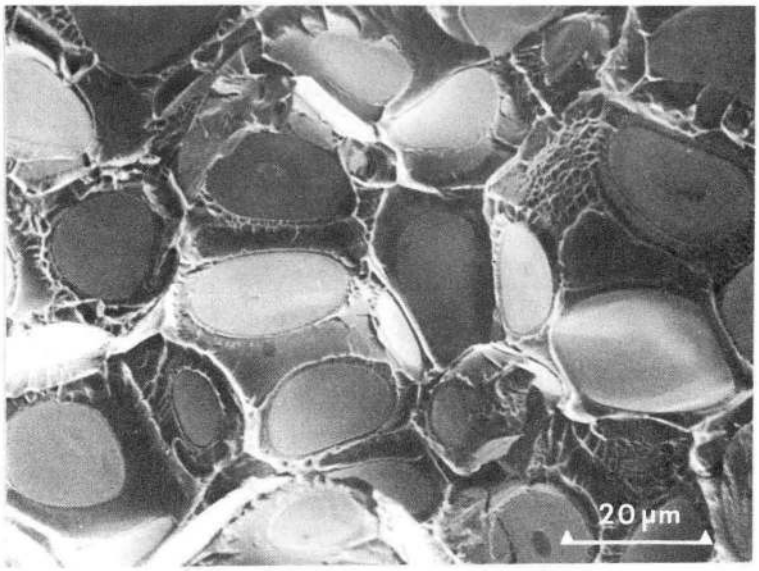

Fig. 3

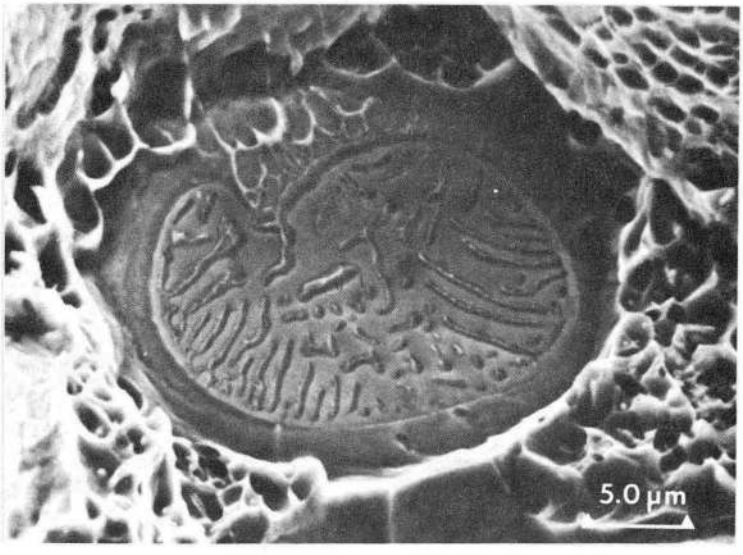

Fig. 4

XBB 855-4069

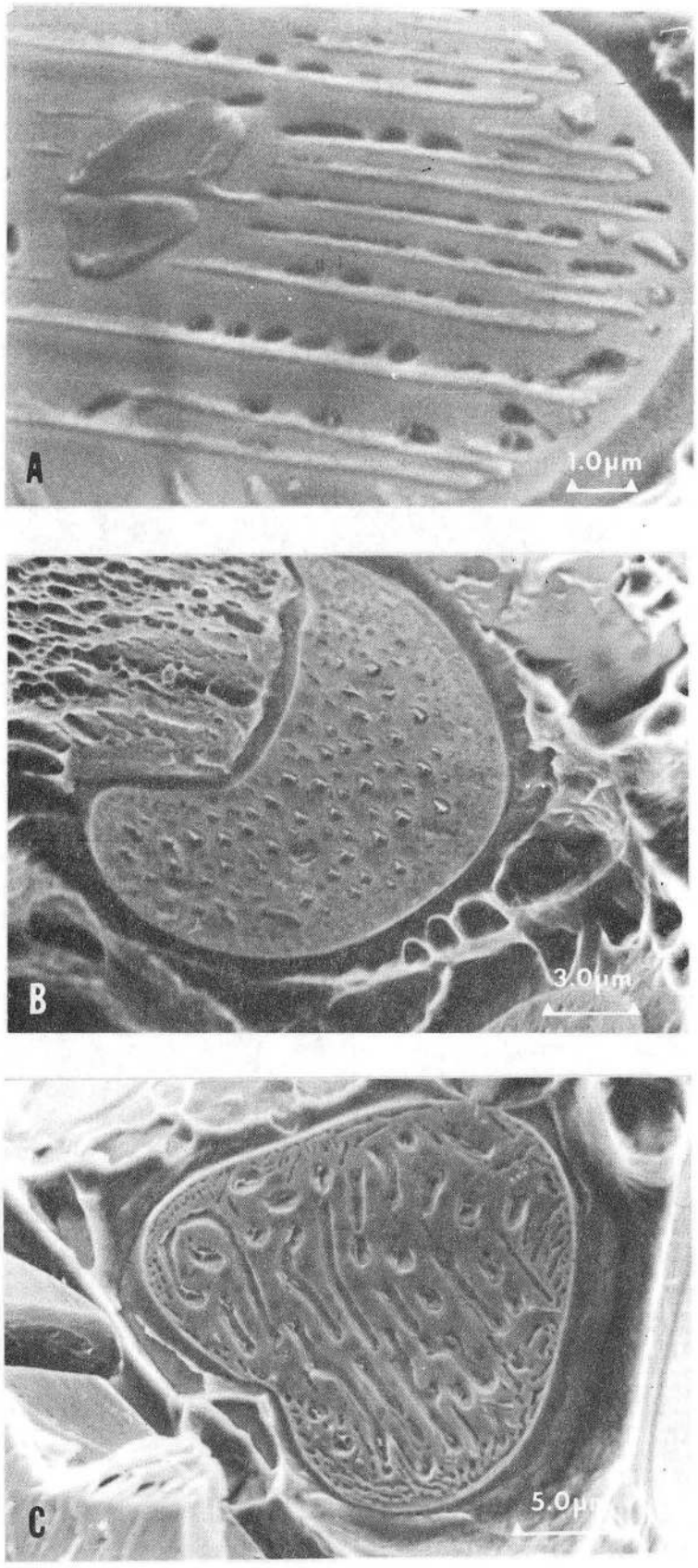

Fig. 5

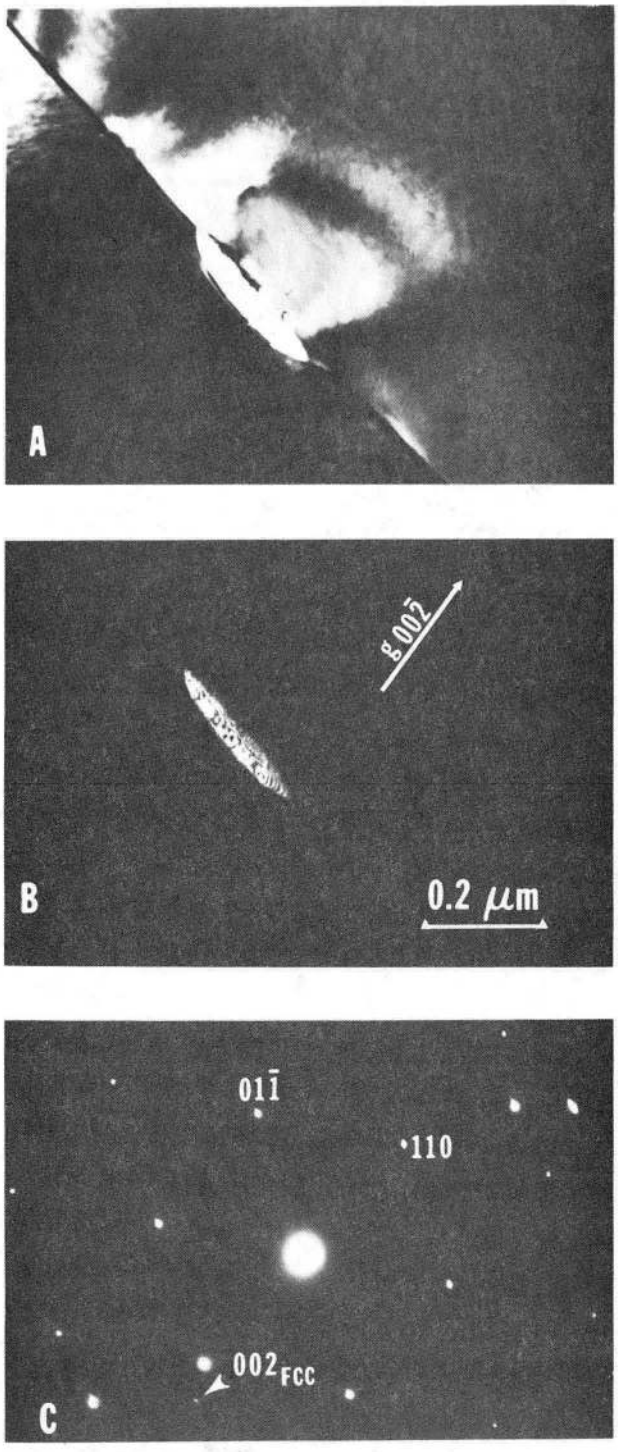

Fig. 6

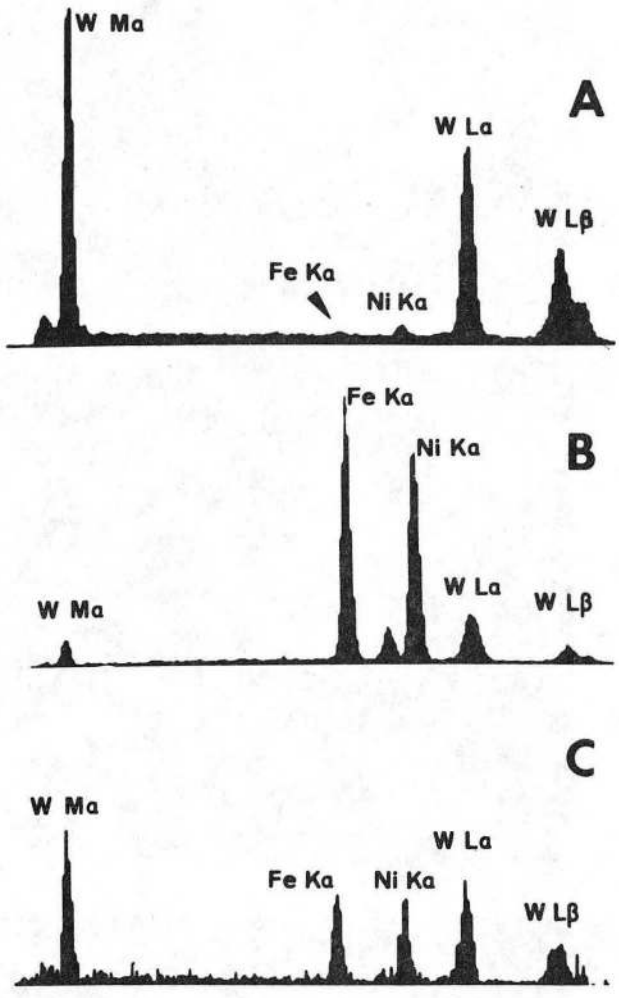

Fig. 7

XBB 855-4072

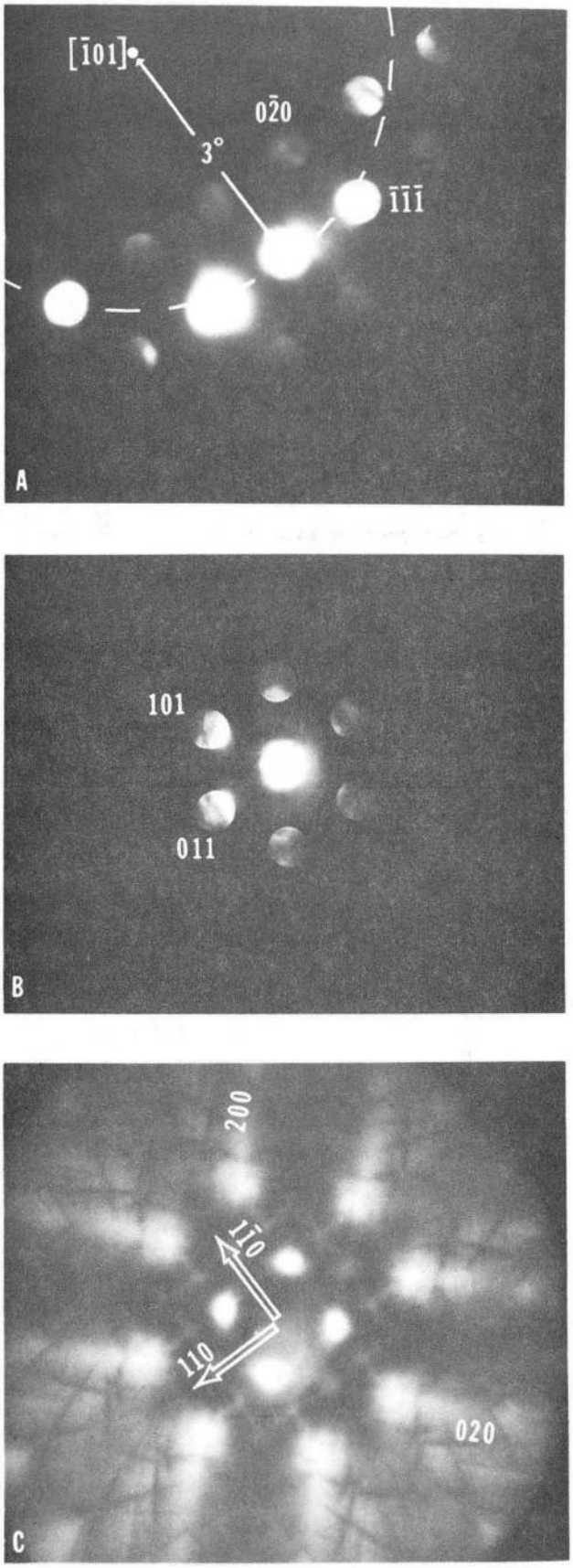

Fig. 8 XBB 855-4073

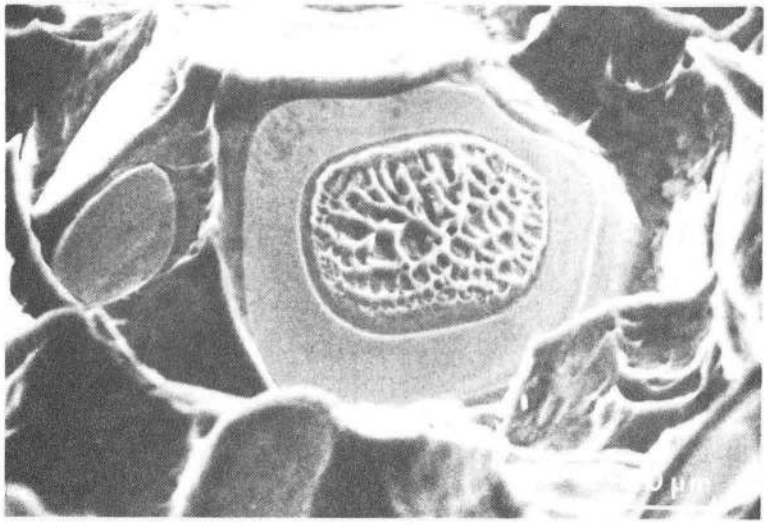

Fig. 9

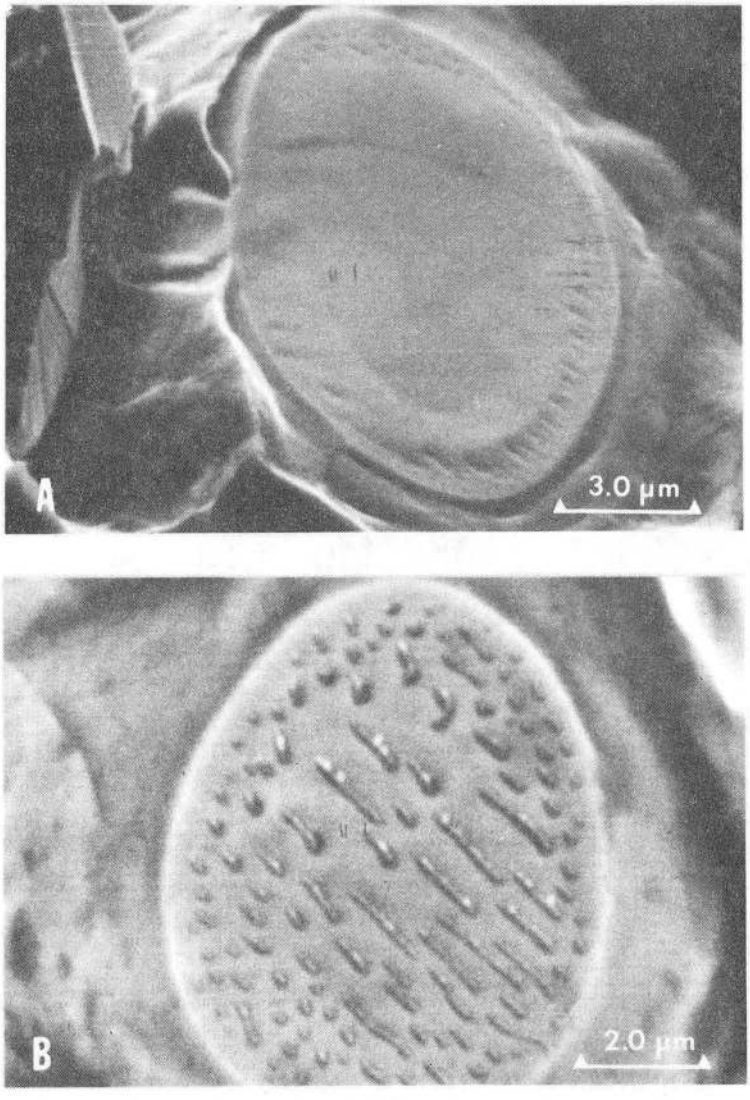

Fig. 10

XBB 855-4068

This report was done with support from the Department of Energy. Any conclusions or opinions expressed in this report represent solely those of the author(s) and not necessarily those of The Regents of the University of California, the Lawrence Berkeley Laboratory or the Department of Energy.

Reference to a company or product name does not imply approval or recommendation of the product by the University of California or the U.S. Department of Energy to the exclusion of others that may be suitable.

LAWRENCE BERKELEY LABORATORY
TECHNICAL INFORMATION DEPARTMENT
UNIVERSITY OF CALIFORNIA
BERKELEY, CALIFORNIA 94720